PHYSICAL REVIEW B VOLUME 56, NUMBER 14 1 OCTOBER 1997-II

Room-temperature dipole ferromagnetism in linear-self-assembling mesoscopic Fe particle arrays

Akira Sugawara* and M. R. Scheinfein
Department of Physics and Astronomy, Arizona State University, Tempe, Arizona 85287-1504
(Received 15 May 1997)

Quasi-one-dimensional, nanometer-diameter Fe particle arrays have been prepared by self-organized shadow growth on regularly faceted NaCl (110) surfaces. A room-temperature dipole-ferromagnetic phase was observed for linear arrays of Fe particles with radii larger than 2.5 nm. Surface magneto-optic Kerr magnetization curves indicate easy-axis alignment along the rows of particles. Remanence and coercivity were strong functions of particle diameter and linear island density. Experimental results are compared with Monte Carlo micromagnetics calculations, which, with no free parameters, reproduce the experimental observations. [S0163-1829(97)50438-3]

Magnetic particle systems are ideal for studying interactions and phase transitions,[1] and are also of interest for application to high-density magnetic storage devices. Recent experiments in surface and low-dimensional magnetism have focused on the properties of surfaces and small particles in order to explore the structure and dynamics of interactions at small length scales. Advanced synthesis methods for the preparation of transition-metal nanoclusters,[2] ordered nanoscale dot-arrays,[3] nanostructured magnetic-networks,[4] submicron[5] and nanometer width wires,[6] and random two-dimensional arrays[7] allow new and unusual magnetic phases to be explored. Although the Néel and Brown[8] theories for relaxation in isolated magnetic particles predict relaxation times that are less than microseconds for 6-nm- (bulk-anisotropy) diameter Fe particles at room temperature, closely packed mesoscopic linear arrays can be remanent and coercive (ordered).[9] Long-range interactions have been studied by ferromagnetic resonance,[10] Mössbauer spectroscopy,[9,11] mean field calculations[12] and Monte Carlo simulations.[7] Identifying the mechanism underlying the interactions is facilitated by the preparation of $3d$-transition metal islands in and on insulators like SiO_2 (Ref. 10), MgO (Ref. 10), and CaF_2 (Ref. 7), which guarantees that particles do not couple through electronic states in the substrate. Here, we report on the observed and computed magnetic properties in linear self-assembling arrays of nanometer-diameter Fe particles. The formation of linear arrays intrinsically breaks the symmetry in the interaction Hamiltonian, thereby stabilizing long-range order. Self-assembly[6,13] is used to form rows of closely packed ($2.1\times10^{12}/\mathrm{cm}^2$) nanometer-diameter Fe islands on an amorphous, insulating substrate (SiO). Self-assembly[13] facilitates the fabrication of macroscopic (3 mm×3 mm) arrays, which would take prohibitively long to define using an electron-beam or scanning-tunneling microscope-based lithography (e.g., Ref. 3). The Fe island radius, island density, the width and separation of the linear island arrays can be varied experimentally in the self-assembled growth process for exploring new magnetic phases. Here, we demonstrate how particle diameter in linear magnetic island arrays can be varied to establish a dipole-induced ferromagnetic state above room temperature.

The linear self-assembling arrays of nanometer-diameter Fe particles are prepared in UHV (2.0×10^{-10} mbar). A schematic depicting the deposition process is shown in Fig. 1. A polished and H_2O-etched single crystal of NaCl (110) is annealed *in situ*. Regular (nano) grooves result when {100} planes form (facet). This reduces the surface free energy by reducing the area of high-energy (110) planes.[13] The spacing of the grooves is a function of the annealing temperature and time. Ten minutes of annealing at 380 °C produce an average trough-to-trough groove spacing of 40 nm. The Fe islands should be randomly oriented and polycrystalline since the goal is to examine the influence of the geometrical particle alignment independent of any intrinsic spin-orbit-induced crystal fields. This is accomplished by coating the NaCl surfaces with an amorphous SiO layer; SiO prevents any epitaxial alignment between the Fe islands and the single crystal NaCl. Fe was deposited from an electron-beam evaporator aligned 70° off the template normal. We show results from three different nominal Fe thicknesses ($t=0.3,0.6,1.0$ nm) grown at a rate of 0.03 nm/min (normal to the terraces) on a substrate heated to 190 °C (thickness as defined in Ref. 7). Fe adatoms agglomerate on SiO in a three-dimensional nucleation and growth mode, where the elevated temperature decreases the nucleation density and liquidlike coalescence is enhanced. The Fe islands are expected to nucleate in the narrow bands exposed to the Fe flux, which here comprise 27% of the ridge-to-ridge distance (10 nm). After Fe deposition, the surface was covered with a 10-nm SiO passivation overlayer.

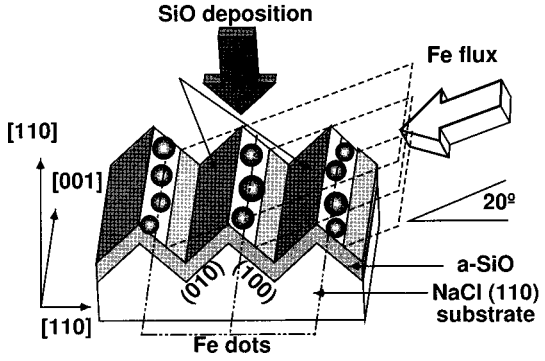

FIG. 1. Schematic depiction of the preparation of self-assembling nanometer-diameter arrays of Fe islands (see text).

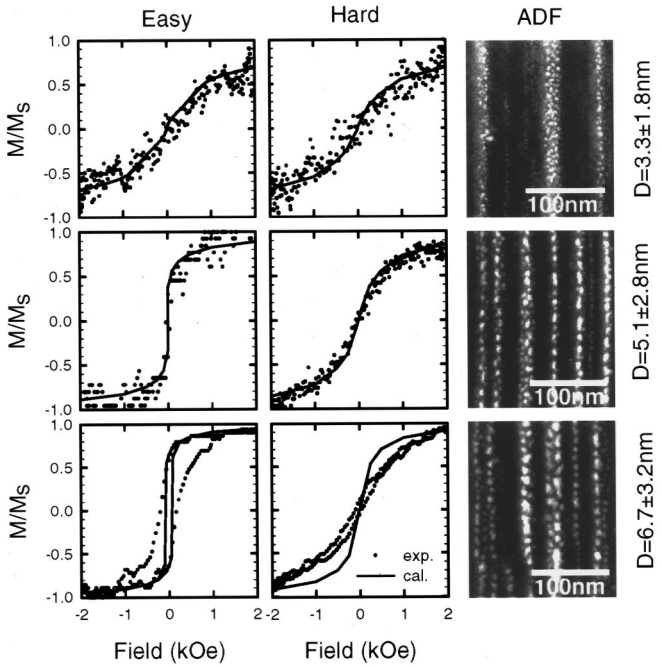

FIG. 2. Magnetic and structural properties of linear arrays of Fe particles of nominal diameter $D=3.3$ nm (top row), 5.1 nm (middle row), and 6.7 nm (bottom row). SMOKE hysteresis loops taken along the easy direction, along the wire (left most column), and perpendicular to the wire, the hard direction, (center column) are shown with solid symbols. The Monte Carlo micromagnetics simulated hysteresis loops are plotted with solid lines. ADF-STEM images of each linear array are shown (right most column) for each nominal particle size.

The microstructure in the linear arrays was examined using conventional transmission electron microscopy, TEM (Topcon EM-002B) and high resolution annular dark-field scanning transmission electron microscopy, ADF-STEM (VG HB-501). Results are given in Fig. 2. The column of images on the right-hand side displays ADF-STEM images of ultrafine particle arrays, with the different (nominal) island diameters indicated. The separated and distinct islands are seen in bright contrast and are aligned parallel to the nanogrooves. Electron diffraction patterns, formed from irradiating large numbers of Fe islands, showed that these islands were randomly oriented polycrystalline bcc Fe. No iron oxide phases were detected. Particles along the lines are clearly separated, and the large interline distance is clearly visible. Typically, lines of particles have a length of 1–10 μm; the aspect ratio is about 100:1. The intermediate contrast between particles results from fluctuations in the SiO underlayer and overlayer thicknesses, and is not related to the Fe. No particle-to-particle crystalline orientation, and no interparticle lattice fringes (bridges) were detected in HRTEM images (not shown). Particle size statistics were obtained by image analysis of several 200×200 nm^2 areas for each film. The particle size statistics are summarized in Table I.

The microstructural evolution driving the formation of the linear arrays is dominated by the high Fe island nucleation density ($>2\times10^{12}$ cm^{-2}) in areas exposed to the Fe flux. The initial distance between nuclei (<7 nm), and the initial island diameter (<2 nm) is smaller than the width of the

TABLE I. Average particle diameter (mean diameter of island-size distribution), island density and interparticle spacing for the Fe particle arrays grown at 190 °C. The nucleation density is normalized to the area exposed to Fe flux, i.e., the array wire width.

Thickness (nm)	Diameter (nm)	Density (nm^{-2})	Spacing (nm)
0.3	3.3 ± 1.8	0.0216	6.8
0.6	5.1 ± 2.8	0.0136	8.6
1.0	6.7 ± 3.2	0.0118	9.2

area exposed to the Fe flux. Several islands can nucleate across the area exposed to the Fe flux. A small amount of Fe might escape from the flux zone due to the adatom concentration gradient formed at the shadow edge. However, this effect appears to be negligible since most adatoms are effectively captured by pre-existing islands. At later stages of growth at 190 °C substrate temperatures, liquidlike coalescence of smaller islands keeps the Fe island perimeters circular (ADF images in Fig. 2). Elevated substrate temperatures round the Fe island surface quickly enough to reduce the surface-energy penalty caused by two neighboring islands that are touching. In contrast, at room temperature, thin wire arrays are formed[6] at an early stage because of slow Fe self-diffusion on the surface. Since the Fe island diameter is on the same order as the terrace width in $D=6.7$ nm case, the microstructure approaches a one-dimensional linear particle array.

The magnetic properties of the arrays were measured *ex situ* at room temperature using the longitudinal magneto-optical Kerr effect (SMOKE).[14] In Fig. 2, results are shown for linear arrays of Fe particles of nominal diameter $D=3.3$ nm (top row), 5.1 nm (middle row), and 6.7 nm (bottom row). Experimental SMOKE hysteresis loops are shown with solid symbols. Loops were taken along the easy direction, along the wire array (left most column), and perpendicular to the wire array, in the hard direction (center column). Kerr loop acquisition times were on the order of seconds to ensure that equilibrium magnetization configurations were measured. The computed hysteresis loops from Monte Carlo micromagnetics[7] simulations are plotted with solid lines.

Monte Carlo models were used to evaluate the magnetic properties of the linear arrays as a function of particle radius and density[7,15] because the Monte Carlo method rigorously accounts for fluctuations. Simulations used periodic boundary conditions, and between 200 and 400 islands randomly arranged into 3 to 5 wires. The model employs an all-orders interparticle interaction Hamiltonian.[7] As input, the model uses the bulk saturation magnetization value, an adjustable externally applied field and the experimental-size distribution of Fe islands given in Table I. The average island diameter is the mean diameter of the island-size distribution. The variation in the island diameter is the standard deviation of the Gaussian fit to the island-size distribution. The slightly irregular experimental island shapes are approximated by cylinders. The cylindrical approximation is justified because there is no orientational order in the films (except the lines) and the intraisland demagnetization fields due to random individual island orientation averages out over the entire film surface. Hysteresis loops are calculated by finding an equi-

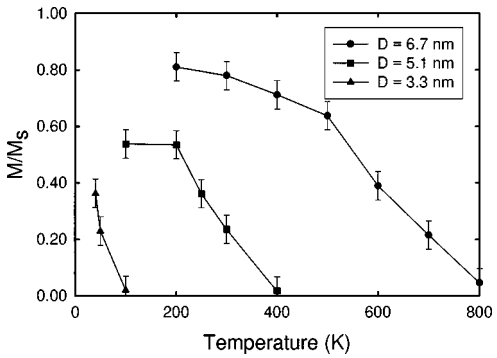

FIG. 3. Order parameter ($M_{\text{along wire}}/M_s$) as a function of temperature and nominal Fe island diameter computed from Monte Carlo micromagnetics.

librium magnetization distribution for an externally applied field value. The magnetization accumulators are reset, the external field value changed, and the previous final magnetization state is preserved as the initial distribution for the next Monte Carlo cycle.

Figure 3 shows the computed normalized magnetization as a function of temperature for the three distributions of islands given in Table I and shown in Fig. 2. The ordering temperature increases with increasing particle diameter as in the two-dimensional random array case.[7] Increasing the number of lines and changing the particle distribution for alternative random seeds produce a 10% variation in the remanence, as indicated by the error bars in Fig. 3. In contrast to the two-dimensional case, the linear arrays order globally rather than locally. This demonstrates that the linear particle arrays order ferromagnetically due to interparticle magnetostatic dipole fields. This is solely due to the symmetry breaking in the geometric structure of the array. For particles of the appropriate size and proximity, room temperature dipole ferromagnetism can be observed. If only bulk anisotropy were present, the arrays would be superparamagnetic at room temperature. Interface anisotropy, which can be orders of magnitude larger than volume anisotropy in thin film systems, has no preferred in-plane orientation and thus cannot be responsible for the long-range order. With typical demagnetization factors of $\frac{1}{2}$ for cylinders in-plane, the stray fields external to the particles can be as high as 10 kOe, with stray field decay lengths set by the particle diameter. The close proximity of the particles forces neighboring particles to lie in each others (large) stray field resulting in long-range order.

A transition to a room temperature, remnant and coercive ferromagnetic state is observed with increasing island diameter (Fig. 2). The easy axis hysteresis loop for $D=5.1$ nm shows an abrupt jump in both the experimental ($H_c<5$ Oe, our experimental resolution limit) and computed ($H_c<1$ Oe) loops. Figure 3 shows that this array is just at the transition to its ordered state at room temperature. The larger islands, $D=6.7$ nm, show easy axis remanence and coercivity in both measured and computed hysteresis loops. The predictive value of the model with no free parameters is evident in Fig. 2. Dipole ferromagnetically ordered films have an easy axis along the wire since the shape anisotropy in that direction is small. Since the particles have no preferential crystallographic orientation in the film plane, magnetocrystalline anisotropy is also negligible. Therefore, the anisotropy that orders the array is ascribed to the strong magnetic interaction between self-aligned particles.

We have fabricated mesoscopic linear arrays of Fe particles whose size and spacing allow them to couple through the interparticle magnetostatic field and order ferromagnetically, even at room temperature. The experimentally determined magnetic properties of these arrays were compared to those predicted by a Monte Carlo micromagnetics simulation with no free parameters. The computation predicts global ordering at room temperature through dipole fields, and the computed hysteresis loops accurately reproduce the results of the experiment.

We are indebted to G. Hembree and S. Coyle for technical support and valuable discussions. We have also benefited from valuable discussions with K. Schmidt and J. Venables. This work was supported by the Office of Naval Research under Grant No. N00014-93-1-0099. The microscopy was performed at the Center for High Resolution Electron Microscopy at Arizona State University. A.S. was supported by JSPS.

*Present address: JAIST, 1-1 Asahi-dai, Tatsunokuchi, Ishikawa, 923-12, Japan.

[1] D. C. Mathis, *The Theory of Ferromagnetism II* (Springer-Verlag, Berlin, 1985); H. E. Stanley, *Introduction To Phase Transitions and Critical Phenomena* (Oxford University Press, London, 1971).

[2] C. P. Gibson and K. J. Putzer, Science **265**, 1338 (1995).

[3] T. Takeshita, Y. Suzuki, H. Akinaga, W. Mizutani, K. Tanaka, T. Katayama, and A. Itoh, Appl. Phys. Lett. **68**, 3040 (1996); M. Hehn, K. Ounadjela, J.-P. Bucher, F. Rousseaux, D. Decanini, B. Bartenlian, and C. Chappert, Science **272**, 1782 (1996); S. Y. Chou, P. R. Krauss, and L. Kong, J. Appl. Phys. **79**, 6101 (1996); R. D. Gomez, M. C. Shih, R. M. H. New, R. F. Pease, and R. L. White, *ibid.* **80**, 342 (1996); S. Gidar, J. Shi, P. F. Hopkins, K. L. Chapman, A. C. Gossard, D. D. Awschalon, A. D. Kent, and S. von Molnàr, Appl. Phys. Lett. **69**, 3269 (1996).

[4] J. A. Barnard, H. Fujiwara, V. R. Inturi, J. D. Jarratt, T. W. Scharf, and J. L. Weston, Appl. Phys. Lett. **69**, 2758 (1996).

[5] A. O. Adeyeye, G. Lauhoff, J. A. C. Bland, C. Daboo, D. G. Hasko, and H. Ahmed, Appl. Phys. Lett. **70**, 1046 (1997).

[6] A. Sugawara, S. T. Coyle, G. G. Hembree, and M. R. Scheinfein, Appl. Phys. Lett. **70**, 1043 (1997).

[7] M. R. Scheinfein, K. E. Schmidt, K. R. Heim, and G. G. Hembree, Phys. Rev. Lett. **76**, 1541 (1996); K. R. Heim, G. G. Hembree, K. E. Schmidt, and M. R. Scheinfein, Appl. Phys. Lett. **67**, 2878 (1995).

[8] L. Néel, Ann. Geophys. **5**, 99 (1949); A. Aharoni, *Introduction To The Theory Of Ferromagnetism* (Oxford Science, Oxford, 1996).

[9] S. Mørup, Phys. Rev. Lett. **72**, 3278 (1994); S. Mørup and G. Christiansen, J. Appl. Phys. **73**, 6955 (1993); S. Mørup, Hyperfine Interact. **60**, 959 (1990); S. Mørup, P. H. Christensen, and B. S. Clausen, J. Magn. Magn. Mater. **68**, 160 (1987); S. Mørup, M. B. Madsen, J. Franck, J. Villadsen, and C. J. W. Koch, *ibid.* **40**, 163 (1983).

[10] W-N. Wang, Z-S. Jiang, and Y-W. Du, J. Appl. Phys. **78**, 6679

(1995); S. Matsuo, T. Matsuura, I. Nishida, and N. Tanaka, Jpn. J. Appl. Phys., Part 1 **33**, 3907 (1994).

[11] S. Linderith, L. Balcells, A. Labarta, J. Tejada, P. V. Hendriksen, and S. A. Sethi, J. Magn. Magn. Mater. **124**, 269 (1993).

[12] M. El-Hilo, K. O'Grady, and R. W. Chantrell, J. Magn. Magn. Mater. **114**, 295 (1992).

[13] A. Sugawara, Y. Haga, and O. Nittono, J. Magn. Magn. Mater. **156**, 151 (1996).

[14] Z. J. Yang and M. R. Scheinfein, J. Appl. Phys. **74**, 6810 (1993).

[15] N. Metropolis, A. W. Rosenbluth, M. N. Rosenbluth, A. H. Teller, and E. Teller, J. Chem. Phys. **21**, 1087 (1953).